

AD-A250 666



(2)

OFFICE OF NAVAL RESEARCH

GRANT NO. N00014-91-J-1447
R&T CODE 414044

Technical Report No. 20

TRIISOPROPYLINDIUM: DECOMPOSITION STUDY AND USE FOR
LOW TEMPERATURE GROWTH

by

C. H. CHEN and G. B. STRINGFELLOW

S DTIC
ELECTED
MAY 27 1992
A D

Prepared for Publication
in the
Journal of Crystal Growth

University of Utah
Dept. of Materials Science & Engineering
Salt Lake City, UT 84112

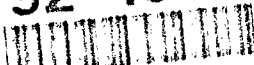
20030220184

May 22, 1992

Reproduction in whole or in part is permitted for any purpose of the
United States Government

This document has been approved for public release and sale; its
distribution is unlimited

92-13835



92 5 26 050

Triisopropylindium: Decomposition Study and
Use for Low Temperature Growth of InAs

C.H. Chen and G.B. Stringfellow

Department of Materials Science and Engineering
University of Utah
Salt Lake City, UT 84112

R.W. Gedridge, Jr.

Chemistry Division
Research Department
Naval Air Warfare Center
China Lake, CA 93555

Accession for	NTIS GRA&I	DTIC TAB	UDC
Justification			
By			
Distribution			
Availability			
Dist	Avail	Special	
A-1			

...1...



Abstract

The organometallic vapor phase epitaxial (OMVPE) growth of In-containing III-V semiconductors typically uses trimethylindium (TMI_n). However, TMI_n suffers from several problems. First, it is well known that the effective vapor pressure of solid TMI_n changes with time because of changes in the surface area. Secondly, TMI_n decomposes slowly for temperatures lower than 400 °C in an atmospheric pressure OMVPE reactor; it is too stable for some low-temperature applications. In addition, it causes carbon contamination, especially at low temperatures, due to the CH₃ radicals. Thus, there is a need for new In precursors that are liquids at room temperature and do not contain CH₃ radicals. This work reports the first decomposition and OMVPE growth studies for a newly developed indium source, triisopropylindium (TIPIn). The decomposition study was carried out in an isothermal flow tube reactor with the reaction products analyzed using a mass spectrometer. The temperature for 50% decomposition is ~110 °C for TIPIn in a He ambient. This is about 200 °C lower than that for TMI_n under similar conditions. The mass spectroscopic peaks occur at m/e=39, 42, 43, 71, and 86, indicating that the major product for TIPIn decomposition is C₆H₁₄. This suggests that TIPIn decomposes by homolysis, producing C₃H₇ radicals that recombine to produce C₆H₁₄. The OMVPE growth study was carried out in an atmospheric pressure OMVPE reactor in H₂ with AsH₃ as the As source. InAs epilayers with good surface morphologies were obtained for temperatures as low as 300 °C at a V/III ratio of 460. The necessary V/III ratio increases as the growth temperature is decreased, due to the incomplete decomposition of AsH₃ at low temperatures. The less reactive C₃H₇ radicals from TIPIn pyrolysis produce far less carbon in the solid than the more reactive CH₃ radicals produced by TMI_n pyrolysis. A

disadvantage of TiPIn is the low growth efficiency, due to parasitic reactions. Thus, it appears that TiPIn may be best suited for low pressure OMVPE or, particularly, for chemical beam epitaxy.

1. INTRODUCTION

In the early development of organometallic vapor phase epitaxy (OMVPE), the growth of In-containing alloys was plagued by parasitic reactions between the most common precursor, triethylindium (TEIn), and the group V hydride sources [1]. Later, it was found that parasitic reactions were reduced using low reactor pressures [2]. The problem was finally resolved when trimethylindium (TMI_n) was introduced as the indium precursor [3, 4]. Today, high quality indium-containing alloys are routinely produced with high growth efficiencies [5].

However, some problems still exist with the use of TMI_n: (1) OMVPE users have long recognized the variable vaporization rate of solid TMI_n. That is, the effective TMI_n vapor pressure decreases after about 40% of usage, presumably due to a decreased surface area caused by recrystallization of TMI_n inside the bubbler [6, 7]. To alleviate the problems, a special sublimer design is necessary [7]. (2) The methyl radicals produced during TMI_n pyrolysis are a likely source for carbon contamination. For example, it has been documented that the methyl radicals from trimethylgallium (TMGa) and trimethylarsine pyrolysis lead to carbon contamination in GaAs as an acceptor impurity [8-10]. For TMI_n, the result has been less definitive [11] because of the relatively low carbon concentrations for normal growth conditions [5]. Recently, the question has been clearly resolved for the growth of InAs at low temperatures, where the carbon concentrations are much higher [12, 13]. For InAs epilayers grown using TMI_n and AsH₃, the carbon concentration detected by secondary ion mass spectroscopy (SIMS) increased as the growth

temperature was reduced [12], with carbon concentrations being more than 10^{19} cm^{-3} at 300 °C [12].

In addition to the above problems, TMIn decomposes too slowly for the growth of InAsBi at very low temperatures (<300 °C) [12]. Recently, Bi concentrations as high as 6% have been incorporated into InAs to reduce the energy bandgap of InAs into the 12 μm range [12]. Thus, InAsBi and InAsSbBi become attractive alternative materials for far infrared device applications. However, it is found that growth temperatures as low as 275 °C are necessary in order to incorporate 6% Bi into InAs. At this low growth temperature, TMIn decomposition is not complete [14] so the growth rates of InAs and InAsBi are unacceptably low [12].

This discussion indicates that the development of other indium sources would be beneficial. One possible replacement is ethyldimethylindium (EDMIn) [6, 12, 15]. Since it is a liquid at room temperature, it does not have the problems associated with a variable transport rate. Although no problems have been reported using EDMIn for OMVPE growth [12], it is not certain how ligand exchange reactions [16] affect the final molecules transporting to the crystal growth surface. Moreover, EDMIn has problems with carbon contamination at low temperatures [12], due to the presence of methyl groups. Thus, there remains a need for other indium precursors.

In this work, we report the results of the first study of triisopropylindium $[(\text{C}_3\text{H}_7)_3\text{In}, \text{TIPIn}]$ as a possible TMIn replacement for OMVPE growth of In-containing materials. Both decomposition and OMVPE growth results are presented.

2. EXPERIMENTAL

The general procedure for the TiPIn synthesis is as follows. Organic solvents were distilled under Ar from sodium/benzophenone. Synthesis was carried out under purified Ar using inert atmosphere techniques. Reaction flasks were wrapped in aluminum foil to minimize exposure to light. Air- and moisture-sensitive materials were transferred inside a N₂-filled Vacuum Atmospheres glove box. InCl₃ (99.999% metal basis) was purchased from Alfa and used as received. (i-Pr)MgCl was purchased from Aldrich Chemical Company and used as received. Nuclear Magnetic Resonance (NMR) spectra were recorded on C₆D₆ solutions with an IBM NR-80 spectrometer.

TiPIn was synthesized by reaction of InCl₃ with 3.5 equivalents of (i-Pr)MgCl in diethyl ether [17]. The diethyl ether was removed under vacuum and the residue was extracted with hexane. After filtration, the solvents were removed by fractional vacuum distillation and the crude product was collected in a liquid N₂ trap. The liquid was then heated to 80-85 °C at 10 torr for 2 hours in the absence of light to remove any traces of solvent. The product was then purified by fractional vacuum distillation two more times (60 °C at 2 torr and 53 °C at 1.2 torr) to yield an air-, heat- and light-sensitive light-yellow pyrophoric liquid. The desired compound was confirmed by ¹H and ¹³C NMR spectroscopy.

The TiPIn vapor pressure has been reported to be [18]

$$\log P(\text{Torr}) = 8.453 - 2665.8/T(\text{K}) \quad (1)$$

This gives a value of 0.32 torr at 25 °C. Our distillation values for TiPIn are 2.0 torr at 60 °C, 1.2 torr at 54 °C, and 0.9 torr at 48 °C. These values are consistent

with the more accurate values from equation (1). In the following, equation (1) was used to calculate the TiPIn partial pressures and V/III ratios.

The decomposition experiments were conducted in an isothermal, flow-tube, SiO_2 ersatz reactor at atmospheric pressure. A detailed description of the apparatus has been published previously [19]. The TiPIn source was held at 23 °C and the carrier gas was He with a flow rate of 40 sccm. Unless otherwise specified, the TiPIn source was purged with He for more than 12 hours before each experiment. For OMVPE growth of InAs, an atmospheric pressure horizontal reactor was used [5]. The arsenic source was 100% arsine. The carrier gas for the sources was palladium-diffused H_2 with a total flow rate of about 2.5 liter/min. Separate stainless steel tubing was used for the group III and V reactants in order to minimize possible parasitic reactions. The mixing of the group III and V reactants occurred immediately before entering the quartz reactor. The typical carrier gas flow rate for TiPIn was 300 cc/min with the bubbler being held at 22 °C. The AsH_3 flow rate was approximately 20 cc/min.

The layers for van der Pauw measurements were grown on semi-insulating InP substrates. The In contacts on the four corners of the rectangular samples were annealed at 300 °C for 1-2 minutes under N_2 . The magnetic field was 5 kG and the sample current was about 10 μA .

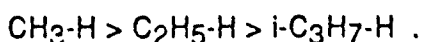
The carbon concentration in the epilayers was measured using a Perkin Elmer 6300 secondary ion mass spectrometry (SIMS). The standard was ion implanted GaAs. A sample was measured twice to ensure the reliability of the measurements.

3. RESULTS AND DISCUSSION

3.1 Decomposition

As mentioned in the experimental section, the TiPIn decomposition study was carried out in a flow tube reactor. The temperature was varied from 50 to 200 °C in 25 °C increments. Fig. 1 shows the results at 50 and 200 °C. The signal intensity is weak as compared to, for example, the decomposition results for TMGa [20]. This is partly due to the low TiPIn vapor pressure at room temperature, giving a low TiPIn partial pressure in the ambient. This is exacerbated by the fact that In sources tend to generally give low signal intensities [21]. No peaks were observed for m/e values between 100 and 300, including the value for the TiPIn parent peak. Comparing the results in Fig. 1 (b) & (c), it is seen that peaks due to TiPIn occur at m/e values of 39, 42, 43, 71, and 86 at 200 °C. The peaks at 42 and 43 can also be resolved for spectra obtained at 125, 150, and 175 °C. So, they are not spurious.

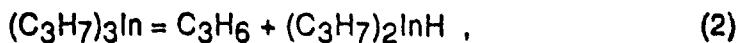
The dependence of peak intensity on temperature is plotted in Fig. 2 for m/e values of 39, 42, 43, and 71. The intensities increase rapidly from 100 to 125 °C and saturate above 125 °C. The results show that the TiPIn decomposes at low temperatures, with a value of T_{50} (temperature for 50% decomposition) of about 110 °C. For comparison, the value of T_{50} obtained for TMIn using similar conditions is about 310 °C [14]. The ease of decomposition is most likely due to the weak In-C₃H₇ bond. It is known that the H-alkyl bond strength decreases in the order [22]:



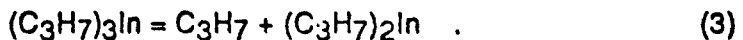
The alkyl-In bond strengths are expected to follow the same order. Thus, TiPIn is expected to decompose at lower temperatures than TMIn.

The intensity for $m/e=43$ is weak at 50°C . If the undecomposed TiPIn makes its way into the mass spectrometer, the principle peak is expected to be due to C_3H_7 at $m/e=43$. This is, indeed, the case for triisopropylantimony [23]. Thus, the principle peak for TiPIn is not positively observed at 50°C . As a result, the intensities at $m/e=39, 42, 43$ come mainly from the decomposition products.

It is difficult to identify the products from Figs. 1 and 2 because only a few peaks are well-resolved. Thus, it is not possible to positively determine the TiPIn decomposition mechanism. One possible reaction pathway is β -hydrogen elimination:



as has been observed to occur for the decomposition of triethylgallium (TEGa) [24], triethylaluminum (TEAl) [25], and triisobutylaluminum (TIBAl) [26]. Another possibility is homolytic fission:



The resulting isopropyl radicals may subsequently participate in disproportionation and recombination reactions:



yielding C_3H_6 , C_3H_8 and C_6H_{14} . The fragmentation patterns for these three species [27] are listed in Table 1 for the m/e values of 39, 42, 43, 71, and 86, the positions of well resolved peaks in this study. From the presence of peaks at

$m/e=71$ and 86, it is clear that C_6H_{14} is produced during TiPIn decomposition. Since the intensities at other peak positions have contributions from C_3H_6 , C_3H_8 and C_6H_{14} , it is not possible to definitively identify the presence of C_3H_6 and C_3H_8 . The fragmentation distribution for C_6H_{16} is plotted in Fig.3 for comparison with the experimental results at 200 °C. The intensity from C_6H_{14} at $m/e=71$ is adjusted to be equal to the experimental result at $m/e=71$. It is seen that the C_6H_{14} fragmentation pattern explains the general features of the experimental result. The intensity at $m/e=39$ may be greater than for C_6H_{14} alone. Thus, it is possible that a small concentration of C_3H_6 and/or C_3H_8 may be produced from TiPIn decomposition. In terms of the reaction mechanism, the results suggest that the reactions (3) and (5) dominate. It is not certain to what degree reactions (2) and (4) contribute to the TiPIn decomposition.

3.2 OMVPE Growth

The OMVPE growth experiments were carried out in a typical OMVPE reactor, as described in the Experimental section. InAs was grown to test the utility of the TiPIn.

The surface morphologies of InAs layers are shown in Fig.4 for growth temperatures of 400, 300, and 260 °C. The V/III ratios are about 460. The surface morphology is very good for the sample grown at 400 °C. Droplets are formed on the surface for the sample grown at 300 °C. For the sample grown at 260 °C, the surface is covered by whiskers and appears to be black to the naked eye. The degradation of surface morphology at lower temperatures is not related to the use of TiPIn, but to the incomplete decomposition of AsH_3 . Since AsH_3 decomposes slowly at low growth temperatures [28], the real V/III ratio at the interface will be much smaller than the input V/III ratio. For the

sample grown at $T_g=260$ °C, the V/III ratio at the interface is probably less than unity. Thus, whiskers are formed, due to well-known vapor-liquid-solid three-phase growth [29, 30]. A similar trend of surface morphology dependence upon growth temperature and input V/II¹ ratio has been reported for OMVPE growth of GaInP using PH₃ [31] and InP using tertiarybutylphosphine [32].

Fig. 5 shows the growth efficiency as a function of growth temperature. The growth efficiency is defined as the growth rate divided by the group III molar flow rate [33]. The epilayer thickness was measured for InAs grown on InP substrates. The results for InAs and InAsBi grown using TMIn in a similar reactor are also shown for comparison [12]. For the growth of InAs using TiPIn at 300 °C, the growth rate is a nearly linear function of the H₂ flow rate (between 0-300 cc/min) through the TiPIn bubbler. It is seen in Fig.5 that the growth efficiency for InAs using TiPIn is only about 700 μm/mole at 500 °C and increases to about 1300 μm/mole at 300 °C. For InAs grown using TMIn and AsH₃, the growth efficiency is on the order of 1×10^4 μm/mole at high temperatures where TMIn is completely decomposed [14]. The low growth efficiency for InAs grown using TiPIn may be due to parasitic reactions between TiPIn and AsH₃. This has been reported to be the case in the growth of InP and GaInAs using TEIn [34]. Because TiPIn has a low value of T_{50} , the low growth efficiency could also be the result of upstream decomposition of TiPIn, resulting in In deposit on the walls. The temperature dependence of the growth efficiency shown in Fig.5 is consistent with either possibility: Lower growth temperatures lead to higher growth efficiencies.

The problem with low growth efficiencies demonstrates the basic difficulty in developing an In precursor for low temperature growth: If the source decomposes at too high a temperature, it is useless for low temperature growth,

since it leads to low growth efficiencies. If the value of T_{50} is too low, decomposition occurs inside the bubbler, on the stainless steel tubing, and/or on the reactor walls upstream of the substrate. This also leads to low growth efficiencies. The low growth efficiency for TiPIn is expected to be alleviated in a low pressure system. It is very unlikely to be a problem in chemical beam epitaxy (CBE). In fact, the stability of TiPIn and the absence of CH_3 radicals would both seem to be favorable for it to be a CBE precursor.

In order to evaluate the electrical properties using the van der Pauw technique, InAs epilayers were grown on semi-insulating InP substrates. The as-grown epilayers are n-type. Fig.6 shows the electron and carbon concentrations plotted versus growth temperature. The results for InAs grown using TMIn and AsH_3 [13] are included for comparison. The electron concentration is about $1 \times 10^{17} \text{ cm}^{-3}$ for samples grown at both 500 and 400 °C. This level of impurity concentration is probably caused by a background impurity present in the TiPIn source. This is not surprising since this is the first bottle of TiPIn ever used for OMVPE growth: It is not of electronic grade. It is expected that this background impurity level can be reduced by further purification of the TiPIn. More significant is the increase in electron concentration when the growth temperature falls below 400 °C.

Recently, InAs has been grown using TMIn and AsH_3 at temperatures as low as 275 °C [12]. It was found that the electron concentration increased as the growth temperature was reduced [12, 13], as shown in Fig.6. The donor impurity has been positively identified as carbon from SIMS measurements [12, 13]. The incorporation of carbon as a donor rather than an acceptor (as for GaAs and AlGaAs) has been explained in terms of the relative bond strengths between carbon and the host group III and V atoms [12]. The trend observed for

TIPIn is similar to that for InAs grown using TMIn. The major difference is that the carbon concentrations for low growth temperatures are much smaller than those for InAs grown using TMIn.

As discussed in Section 3.1, TIPIn decomposes mostly by homolysis, that is, by reactions (3) and (5). Thus, free isopropyl radicals are present on the surface. The less reactive isopropyl radicals are expected to result in less carbon incorporation than for CH₃. On the other hand, if reaction (2) is the dominant pathway, little carbon contamination would be expected because the reaction product is propene which is unlikely to lead to carbon contamination. For example, methane has been demonstrated to be an ineffective dopant for GaAs [35, 36]. In addition, TEGa, which decomposes via the β -hydrogen elimination reaction, has been used to grow GaAs and AlGaAs with very low levels of carbon contamination [37].

4. Conclusions

TIPIn has been investigated as a possible replacement for TMIn in OMVPE growth. From the decomposition results, it is found that TIPIn decomposes with a value of T₅₀ of about 110 °C, approximately 200 °C lower than the value for TMIn under similar conditions. The major product is identified as C₅H₁₄. The decomposition results suggest that the TIPIn decomposes mainly by homolysis, followed by recombination of the C₃H₇ radicals. The growth results show that good surface morphology InAs can be obtained provided that the V/III ratio is sufficiently high. The required V/III ratio has to be increased as the growth temperature is lowered because less AsH₃ is decomposed at lower temperatures. Because the isopropyl radicals are much

less reactive than methyl radicals, the carbon concentration is reduced by several orders of magnitude when TiPIn replaces TMIn or EDMIn.

5. Acknowledgements

The authors would like to thank S.H. Soh and K.T. Huang for assisting with room temperature van der Pauw measurements and Dr. Ray Menna at the David Sarnoff Research Center for doing the SIMS measurements. Financial support of the this work is provided by the Army Research Office, Office of Naval Research, and Office of Naval Technology.

6. References

1. H.M. Manasevit and W.I. Simpson, *J. Electrochem. Soc.* **120**, 135 (1973).
2. J.P. Duchemin, J.P. Hirtz, M. Razeghi, M. Bonnet, and S.D. Hersee, *J. Cryst. Growth* **55**, 64 (1981).
3. C.P. Kuo, J.S. Yuan, R.M. Cohen, J. Dunn, and G.B. Stringfellow, *Appl. Phys. Lett.* **44**, 550 (1984).
4. C.C. Hsu, R.M. Cohen, and G.B. Stringfellow, *J. Cryst. Growth* **63**, 8 (1983).
5. C.H. Chen, M. Kitamura, R.M. Cohen, and G.B. Stringfellow, *Appl. Phys. Lett.* **49**, 963 (1986).
6. C.P. Kuo, R.M. Fletcher, T.D. Osentowski, G.R. Trott, and J.E. Fouquet, paper presented at *The Fourth Biennial Workshop on Organometallic Vapor Phase Epitaxy*, October 8-11, 1989, Monterey, California.
7. AKZO Chemicals Inc., *Newsletter*, October, 1991.

8. T.F. Kuech and E. Veuhoff, *J. Cryst. Growth* **68**, 148 (1984).
9. J. van de Ven, H.G. Schoot, and L.J. Giling, *J. Appl. Phys.* **60**, 1648 (1986).
10. R.M. Lum, J.K. Klingert, D.W. Kisker, S.M. Abys, and F.A. Stevie, *J. Cryst. Growth* **93**, 120 (1988).
11. S. Bose, S. Jackson, A. Curtis, and G. Stillman, paper L2 presented at the 18th International Symposium on GaAs and Related Compounds, Sept. 9-12, 1991, held at Seattle, Washington, USA.
12. K.Y. Ma, Z.M. Fang, R.M. Cohen, and G.B. Stringfellow, *J. Appl. Phys.* **70**, 3940 (1991).
13. Z.M. Fang, K.Y. Ma, R.M. Cohen, and G.B. Stringfellow, *Appl. Phys. Lett.* **59**, 1446 (1990).
14. N.I. Buchan, C.A. Larsen, and G.B. Stringfellow, *J. Cryst. Growth* **92**, 591 (1988).
15. K.L. Fry, C.P. Kuo, C.A. Larsen, R.M. Cohen, G.B. Stringfellow, and A. Melas, *J. Electron. Mater.* **15**, 91 (1986).
16. P.D. Agnello and S.K. Ghanhdji, *J. Cryst. Growth* **94**, 311 (1989).
17. B. Neurnuller, *Chem. Ber.* **122**, 2283 (1989).
18. V.K. Vanchagova, A.D. Zorin, V.A. Umilin, *Zh. Obschei. Khim.* **46**, 989 (1976).

19. N.I. Buchan, C.A. Larsen, and G.B. Stringfellow, *Appl. Phys Lett.* **51**, 1024 (1987).
20. In this lab, the intensity for TMGa and some other precursors is on the order of 10^{-9} amperes, about two orders of magnitude higher than that used in Fig.1.
21. TMin tends to deposit more on the reactor walls than TMGa. This reduces the amount of TMin being delivered to the hot zone of the reactor to be pyrolyzed.
22. G.B. Stringfellow, "Organometallic Vapor Phase Epitaxy: Theory and Practice", (Academic Press, New York, 1989), Chapter 2.
23. S.H. Li, C.A. Larsen, G.B. Stringfellow, and R.W. Gedridge, Jr., *J. Electron. Mater.* **20**, 457 (1991).
24. M. Yoshida, H. Watanabe, and F. Uesugi, *J. Electrochem. Soc.* **136**, 677 (1985).
25. W.L. Smith and T. Wartik, *J. Inorg. Nucl. Chem.* **29**, 629 (1967)
26. M.E. Gross, L.H. Dubois, R.G. Nuzzo, and K.P. Cheung, *MRS Symposium proceedings*, Vol.204, pp383
27. F.W. McLafferty and D.B. Stauffer, *The Wiley/NBS Registry of Mass Spectral Data*, (Vol.1, John Wiley & Sons, N.Y., 1989)
28. see Ref.22, Section 4.2.2.1
29. see Ref.22, pp84-86

30. R.S. Wagner, in "Whiskers Technology", edited by A.P. Levitt (Wiley, New York, 1970)
31. J.S. Yuan, M.T. Tsai, C.H. Chen, R.M. Cohen, and G.B. Stringfellow, *J. Appl. Phys.* **60**, 1346 (1986)
32. C.H. Chen, D.S. Cao, and G.B. Stringfellow, *J. Electron. Mater.* **17**, 67 (1988)
33. see Ref.22, Section 1.3
34. C.P. Kuo, Ph.D. Thesis, University of Utah, 1985
35. R.M. Lum, J.K. Klingert, D.W. Kisker, D.M. Tennant, M.D. Morris, D.L. Malm, J.Kovalchick, and L.A. Heimbrook, *J. Electron. Mater.* **17**, 101 (1988)
36. T.F. Kuech, G.J. Scilla, and F. Cardone, *J. Cryst. Growth* **93**, 550 (1988)
37. T.F. Kuech, *Materials Science Reports* **2**, 1 (1987)

Table 1 Fragmentation Patterns for C₃H₆, C₃H₈ and
C₆H₁₄ at several selected m/e values [27]

m/e	C ₃ H ₆	C ₃ H ₈	C ₆ H ₁₄
	(%)	(%)	(%)
39	71.1	17.0	18.49
42	67.7		84.63
43		22.8	100
71			18.94
86			4.1

Note: The percentage is relative to the principle peak intensity
which is taken to be 100 %.

Figure Captions:

Fig. 1 Mass spectroscopic results for TIPIn decomposition: (a) background of the mass spectrometer; (b) TIPIn + He at 50 °C; (c) TIPIn + He at 200 °C.

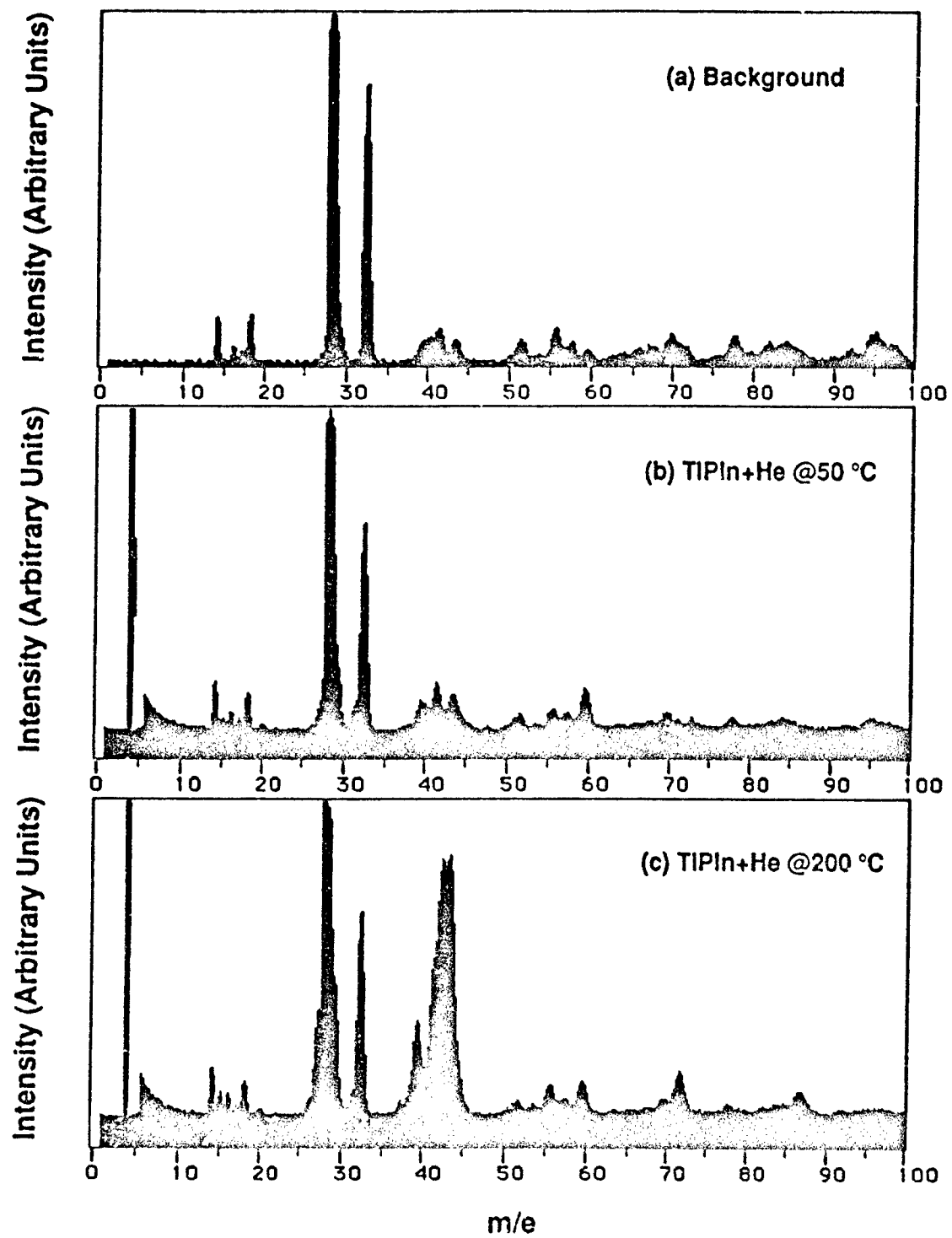
Fig.2 Mass spectral intensities versus temperature at several values of m/e.

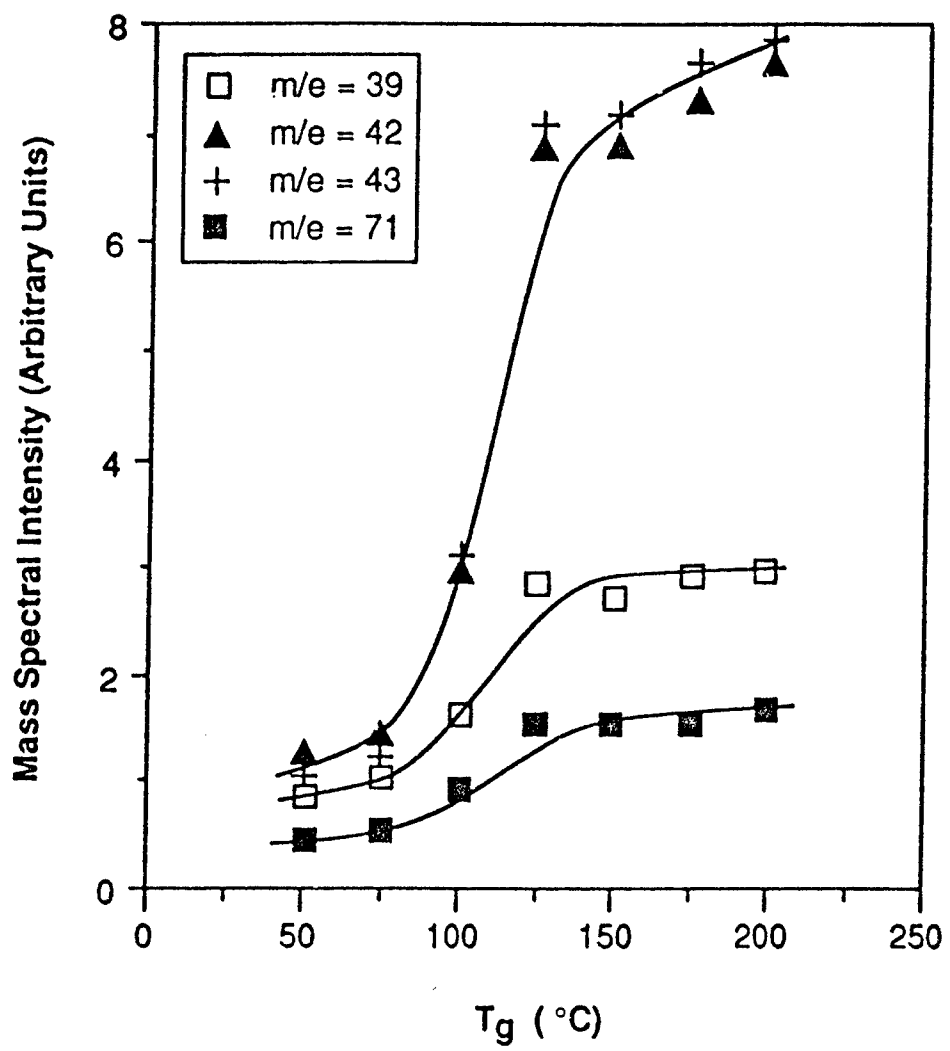
Fig.3 Measured mass spectral intensity distribution at 200 °C compared with that expected for C₆H₁₄ [27].

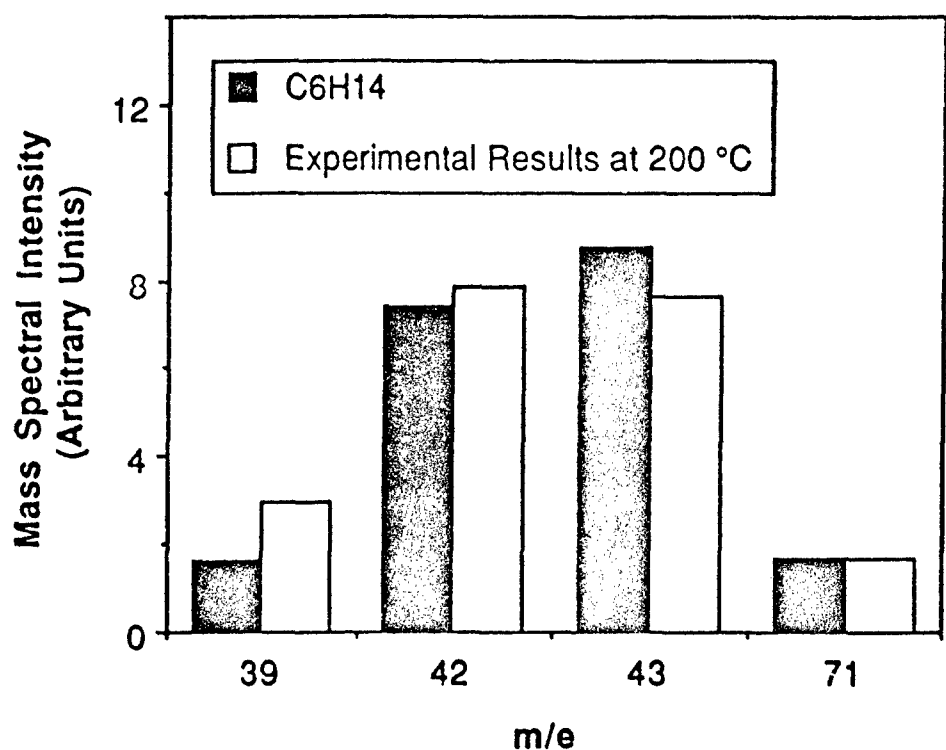
Fig.4 Surface morphologies of InAs layers grown using TIPIn and AsH₃ at 400, 300, and 260 °C with V/III ratios of approximately 461.

Fig.5 Growth efficiency for InAs grown using TIPIn and AsH₃ as a function of growth temperature. The results for InAs and InAsBi grown using TMIn in a similar reactor are also shown for comparison.

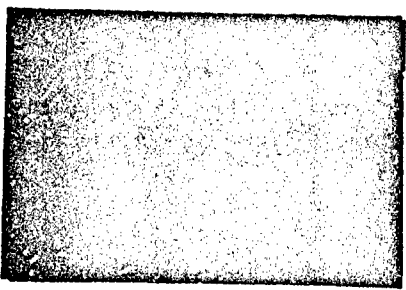
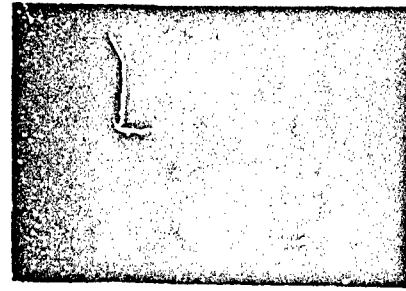
Fig.6 Room temperature electron and carbon concentrations for InAs grown using TIPIn and TMIn as a function of growth temperature. For comparison, the results for InAs grown using TMIn and EDMIn are also shown.







40 μm



Tg = 400 °C
V/III = 461

Tg = 300 °C
V/III = 461

Tg = 260 °C
V/III = 461

